Glycoconjugate Journal (1995) **12**: 113–121

The interaction between wheat germ agglutinin and membrane incorporated glycophorin A. An optical binding study

JEREMY J, RAMSDEN[1]* and CHRISTINE SCHUBERT WRIGHT[2]

[1]*Department of Biophysical Chemistry, Biozentrum, CH-4056 Basle, Switzerland*

[2]*Departments of Biochemistry and Molecular Biophysics and Medicinal Chemistry, Medical College of Virginia, Virginia Commonwealth University, Richmond, VA 23298-0540, USA*

Received 2 May 1994, revised 8 October 1994

A novel integrated optical technique is used to monitor the kinetics of incorporation of glycophorin A (GPA) from solution into a planar dimyristoylphosphatidylcholine–cholesterol bilayer membrane, and the subsequent binding of wheat germ agglutinin (WGA) to the membrane-incorporated GPA. The technique significantly improves the attainable accuracy of kinetic measurements. The number of bound molecules can be determined to a precision of ca ± 80 mol μm^{-2}. Our results show that GPA incorporates spontaneously into the bilayer. Binding of WGA to GPA is optimal in the presence of human serum albumin, and can be reversed by *N*-acetyl-D-glucosamine. The kinetics of the binding are consistent with the presence of two classes of kinetically distinguishable binding sites with association rates of 2.0×10^4 and 9.6×10^2 M^{-1} s^{-1}, and dissociation rates of 2.7×10^{-3} s^{-1} and $< 10^{-5}$ s^{-1}, respectively. A stoichiometry of 4 WGA monomers per GPA monomer was determined as characteristic of the overall binding interaction.

Keywords: lectin receptor binding, adsorption, integrated optics, lipid membrane incorporation

Abbreviations: DMPC, dimyristoylphosphatidylcholine; GlcNAc, *N*-acetyl-D-glucosamine; GPA, glycophorin A; HSA, human serum albumin; NeuNAc, *N*-acetyl-D-neuraminic acid; TE, transverse electric; TM, transverse magnetic; WGA, wheat germ agglutinin.

Introduction

Plant lectins are oligomeric proteins that can specifically bind to glycoconjugate receptors on animal cells and thereby induce biological processes [1–3]. Standard techniques such as electron microscopy, autoradiography and radioactivity counting have traditionally been used to visualize lectin receptors on cell surfaces and estimate association constants. Such methods involve introducing fluorescent or radioactive labels into the lectin molecule in order to determine the number of molecules bound per cell. Due to the structural complexity of cell surface environments, however, interpretation of kinetic data describing these binding events has not been straightforward [4, 5].

Standard bimolecular kinetics are observed when lectins bind to simple oligosaccharides in solution, but lectin-cell binding isotherms have displayed nonlinear behaviour in a wide range of studies. For instances, biphasic Scatchard [6] binding curves obtained for WGA and *Ricinus communis* lectin binding to erythrocytes, and WGA and limulin binding to baby hamster kidney cells, have suggested the presence of two classes of receptors differing in their lectin affinities [7, 8]. As noted by Lis and Sharon [5], association constants reported for lectin-cell binding in the range of $K_a = 10^6 - 10^7$ M^{-1} [4] are several orders of magnitude higher than those for simple mono- and oligosaccharides. In view of the fact that dissociation is very slow, however, the observation that lectin-cell binding is rapidly reversed in the presence of specific monosaccharides is inconsistent with a mechanism in which the simple sugar competes with complex oligosaccharide receptors for lectin binding.

Positive cooperativity has been inferred in a number of studies under conditions of low lectin concentration [9–15]. Recently reported structural evidence based on electron microscopy of lectin-oligosaccharide precipitates [16, 17] and X-ray diffraction studies of crystal complexes [18–20] lends weight to the notion of multivalent lectin-receptor interactions. In these immobilized complexes lectin molecules are crosslinked by bi- and trivalent oligosaccharides forming well-ordered homogeneous two-dimensional lattices. Bhattacharyya and Brewer [17] speculated that these unique modes of crosslinking could be responsible for many of the observed

* To whom correspondence should be addressed.

features of lectin binding to eukaryotic cells, providing increased specificity for the binding process.

The dimeric lectin wheat germ agglutinin (WGA) is a well characterized member of the highly conserved family of disulfide-rich *N*-acetyl-D-glucosamine (GlcNAc)-binding lectins from *Gramineae*. It also recognizes *N*-acetyl-D-neuraminic acid (NeuNAc) present at non-reducing terminal positions of various cell surface carbohydrate moieties [9, 21–25]. WGA binding to erythrocytes is particularly well studied. The sialoglycoprotein glycophorin A (GPA) has been identified as the specific receptor [7, 15]. Glycophorin A is a transmembrane protein with a highly sialylated extracellular domain containing fifteen of the bivalent O-linked type of tetrasaccharide [26, 27] and one N-linked oligosaccharide [28, 29]. The carbohydrate moieties are antigenic determinants as well as receptors for viruses and lectins [30, 31]. Binding isotherms based on isotopic labelling of WGA with ^{125}I [7, 15] indicated the presence of a class of low ($K_a = 10^6$ M^{-1}) and high ($K_a = 1.3 \times 10^7$ M^{-1}) affinity sites at saturation, values which are in the range typical for lectin-cell binding.

WGA is an unusual protein compared with other lectins from well-defined families in that its polypeptide chain is composed of a tandem repeat of four independently folded 43-amino acid segments termed A, B, C, and D [32]. Each domain is stabilized by four invariant disulfide bridges and contains an aromatic amino acid-rich pocket for sugar binding. Although many of the amino acids involved in the binding are conserved, sugar affinities are expected to vary among the four independent sites as a result of the character of the aromatic residues and the extent to which hydrogen bonding assists ligand binding across the dimer interface through two non-conserved polar residues on monomer 2 [18].

In this study, a novel integrated-optical technique is used to follow the kinetics of the binding of WGA to GPA incorporated into a lipid bilayer. The biological properties of GPA assembled into lipid bilayers or liposomes have previously been studied [33–35]. The present method involves the preparation of bilayers deposited on to planar optical waveguides. GPA is incorporated into the bilayer membrane, and exposed to a solution of WGA. The *mode spectrum* of guided waves propagating along the waveguide, characterized by the mode indices *N*, is highly sensitive to the presence of proteins at the membrane surface [36]. The measured shifts in *N*, provided that they are determined accurately enough, can be used to calculate the number of protein molecules at the waveguide surface [36]. The technique is related to other optical methods for probing the surface, such as ellipsometry [37] and scanning angle reflectometry [38]. Integrated optics is more convenient, both in the experimental set-up, which allows a much better time resolution of adsorption kinetics, and in the calculation of the amount of adsorbed protein from the experimentally measured quantity. An additional advantage is that it is unnecessary to attach labels to the molecules.

Experimental

Proteins, lipids and reagents Dimyristoylphosphatidylcholine (DMPC) was purchased from Avanti Polar Lipids (Alabaster, AL), cholesterol (purissimum) from Fluka, and both used without further purification. GPA was purchased from Sigma and appeared to be sufficiently pure as judged from the single band appearing on 12.5% SDS gel. Human serum albumin (HSA) was obtained from Calbiochem (> 99% pure), and WGA isolectin I isolated by CM-sepharose chromatography [39]. The buffer used throughout was 50 mM sodium acetate-acetic acid (analytical grade reagents from Merck), pH 5.6, refractive index n_C=1.331842 at 24.8°C and 632.8 nm. *N*-acetyl-D-glucosamine (GlcNAc) was from Sigma. Water was from a 'Nanopure' (Barnstead, Dubuque, IO) installation.

Preparation of waveguides Planar optical waveguides, consisting of a thin (~ 160 nm) high refractive index layer of $Si_{0.55}Ti_{0.45}O_2$ supported on an optical glass slide 0.5 mm thick, were obtained from Artificial Sensing Instruments, Zurich, Switzerland. The waveguides incorporated a grating coupler (2403 lines per mm). Prior to use these waveguides were cleaned in 2% Hellmanex solution at 60 ± 10°C for 30 min followed by extensive rinsing in distilled water, and overnight storage in the buffer.

Deposition of lipid bilayers A monolayer consisting of DMPC and cholesterol (molar ratio 8:3) was spread on the surface of a laboratory-built Langmuir trough filled with buffer and slowly compressed to a surface pressure of 32 mN m^{-1}. The clean waveguide was lowered rapidly (0.7 mm s^{-1}) and vertically through this compressed floating monolayer. No deposition took place. The waveguide was then slowly (0.14 mm s^{-1}) and vertically raised while maintaining the surface pressure at 32 mN m^{-1}. This resulted in the deposition of a complete DMPC cholesterol monolayer on to the waveguide such that the lipid head groups were oriented towards the waveguide surface. The surface film of water was allowed to evaporate (2–3 min). To complete the lipid bilayer membrane the waveguide was then lowered rapidly (~ 100 mm s^{-1}) and horizontally through the floating monolayer, resulting in the deposition of a second monolayer (see Fig. 1). Experience has shown that the deposition of a phospholipid bilayer requires this combination of vertical (Langmuir-Blodgett) and horizontal (Langmuir-Schaefer) movements, whereas simple fatty acid multilayers require only alternate vertical raising and lowering. The membrane-coated waveguide was then transferred without traversing another air-water interface to the measuring head of an IOS-1 integrated optics scanner (Artificial Sensing Instruments, Zurich, Switzerland). A flow-through cuvette was fixed over the waveguide, which thus formed one wall of the cuvette (Fig. 2). The temperature of the measuring head was maintained at 24.8 ± 0.2°C.

Determination of the mode spectrum The diffraction grating incorporated into the waveguide allows an external light beam

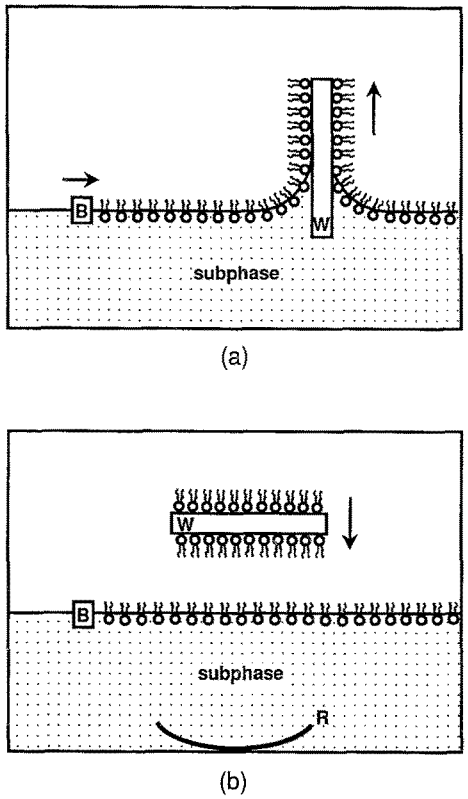

Figure 1. Schematic representation of (a) the Langmuir-Blodgett and (b) the Langmuir-Schaefer techniques for the successive deposition of floating lipid monolayers on to a planar waveguide W. The subphase was the acetate buffer used in all the experiments. B denotes the barrier which is moved to keep the surface pressure constant. The area swept by the barrier movement exactly equals the area of the waveguide on which the lipid is deposited, and by recording this movement the transfer of the monolayer onto W can be monitored. R labels the receptacle in which the waveguide is collected prior to its transfer to the IOS-1 apparatus. General principles of the Langmuir-Blodgett technique for monolayer manipulation can be found in Roberts [37].

to be coupled into the waveguide provided the following condition is fulfilled [41]:

$$N = n \sin \alpha + l\lambda/\Lambda \qquad (1)$$

where N is the index of the guided mode, n the refractive index of air, α the angle of incidence (see Fig. 2), l the diffraction order, λ the wavelength of the light (we used a low-power He-Ne laser emitting at 632.8 nm), and Λ the distance between successive rulings of the grating. In order to determine N, the angle of incidence is varied while recording the power of the light coupled into the waveguide; the peak positions then yield N according to equation (1). This operation is carried out automatically in the IOS-1 instrument. N for two modes, the zeroth transverse electric (TE) and transverse magnetic (TM), sufficient to determine the mass of protein present at the surface, were determined using first-order diffraction ($l = 1$). Initially N was measured with pure buffer in the

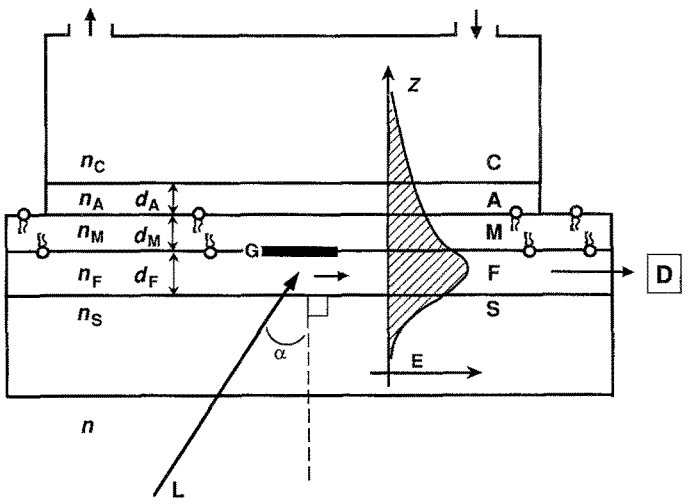

Figure 2. Schematic diagram of the waveguide and cuvette. S, glass support; F, $Si_{0.55}Ti_{0.45}O_2$ film; M, DMPC-cholesterol membrane; A, protein adlayer (GPA bound to the membrane, WGA bound to GPA, etc); C, cover medium (buffer). The refractive indices and thicknesses of the various layers are denoted by n and d respectively. L, external light beam (He-Ne laser $\lambda = 632.8$ nm); G, grating; α, angle of incidence of L on to G; D, detector (photodiode) of the power of light coupled into the waveguide. Also shown (shaded) is the electric field distribution of a zeroth order TE waveguide mode. The evanescent field beyond the confines of the waveguiding layer proper (F) is responsible for the interaction with bound adlayers.

cuvette. From these baseline readings n_F and d_F could be calculated [36, 41]. These quantities are needed later for calculating the mass of bound protein. Subsequently the cuvette was rapidly filled with protein dissolved in buffer solution, and N measured every 15 s or more. To record dissociation, pure buffer then flowed through the cuvette at a rate of 10 $mm^3\ s^{-1}$. A typical series of measured points is shown in Fig. 3. More details of the sequence of adding proteins are given below.

Calculation of mass of bound protein We are essentially concerned with a bound monolayer of protein, either of GPA bound to the membrane or of WGA bound to the membrane-bound GPA, and the bound adlayer A can be characterized by two parameters, its thickness d_A and concentration c_A, and the bound mass Γ is then simply the product of d_A and c_A, i.e. $\Gamma = d_A c_A$. Up to concentrations of 0.4 g cm^{-3} at least, the refractive index of a protein solution is related to its concentration according to [42] $n_A = n_C + c_A\ (dn/dc)$, where the coefficient dn/dc has the value 0.18 $cm^3\ g^{-1}$ for many proteins [42]. With this relation, c_A can be eliminated from the definition of Γ to yield:

$$\Gamma = d_A(n_A - n_C)/(dn/dc) \qquad (2)$$

which shows that to determine Γ, we need to know the two opto-geometrical adlayer parameters n_A and d_A. These can readily be calculated from the mode equations for the zeroth-order TE and TM modes [36, 41]:

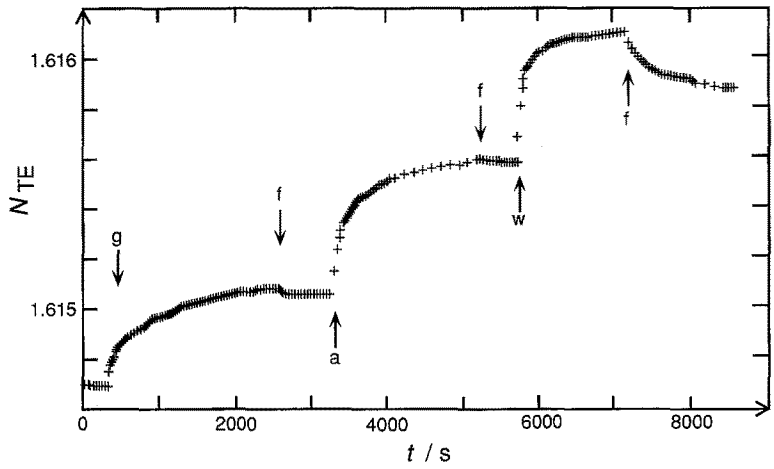

Figure 3. Typical sequence of measured N_{TE}. The arrows correspond to the following steps: g, addition of GPA (50 μg cm^{-3}); f, buffer flowing at 5 mm^3 s^{-1} through the cuvette; a, addition of HSA (50 μg cm^{-3}); w, addition of WGA (50 μg cm^{-3}).

$$\frac{2\pi}{\lambda}\sqrt{n_F^2 - N^2}\left(d_F + d_A\frac{n_A^2 - n_C^2}{n_F^2 - n_C^2}\right)\left[\frac{(N/n_C)^2 + (N/n_A)^2 - 1}{(N/n_C)^2 + (N/n_F)^2 - 1}\right]^{\rho}$$
$$= \arctan\left(\left[\frac{n_F}{n_S}\right]^{2\rho}\sqrt{\frac{N^2 - n_S^2}{n_F^2 - N^2}}\right) + \arctan\left(\left[\frac{n_F}{n_C}\right]^{2\rho}\sqrt{\frac{N^2 - n_C^2}{n_F^2 - N^2}}\right), \quad (3)$$

where n_S = 1.525781 is the refractive index of the support glass and n_C the refractive index of the cover medium (buffer), which we determined using an LI-3 interferometer (Carl Zeiss, Jena, Germany). The parameter ρ equals either 0, for the TE mode, or 1, for the TM mode. Expression (3) therefore represents two equations which can be solved simultaneously to yield from the two measured parameters N_{TE} and N_{TM} the two unknowns d_A and n_A, all other parameters being known, from which Γ can be calculated using equation (2). The experimental error in Γ amounts to about 1 ng cm^{-2}.

Sequence of measurements Following satisfactory deposition of the lipid bilayer on to the waveguide and measurement of the baseline parameters, the cuvette was filled with GPA solution (50 μg cm^{-3}) while continuing to record N in the IOS-1 apparatus. In this way we could follow the incorporation process on-line, as illustrated in Fig. 3. The membrane was subsequently saturated with HSA to optimize the binding interaction between WGA and GPA [35]. Upon addition of the WGA solution further binding took place, the specificity of which was demonstrated by the observation that a subsequent large excess of GlcNAc dissociated WGA from the bilayer. When the HSA step was omitted, nonspecific binding of WGA was observed, which could not be reversed by exposure to GlcNAc (Fig. 6): this nonspecifically bound WGA was, however, dissociated in the presence of 56 mM HCl (this particular concentration was chosen to match the refractive index of the buffer solution).

Several control experiments were carried out to assess the extent to which WGA would interact directly with the bare DMPC-cholesterol bilayer in the absence of GPA, or with a DMPC-cholesterol bilayer on to which HSA had been adsorbed. This is illustrated in Fig. 4. Less WGA was bound, and in neither case could the bound WGA be removed by GlcNAc, but in both cases it could be removed by briefly flushing with 56 mM HCl. The HCl treatment also removed HSA adsorbed to the lipid bilayer.

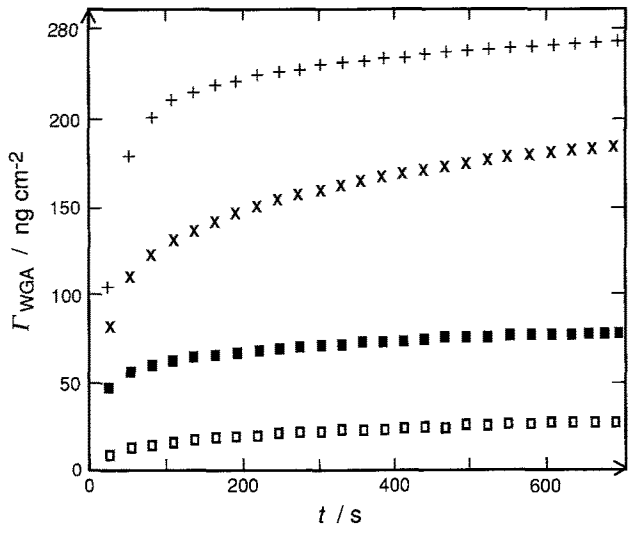

Figure 4. WGA (at a concentration of 50 μg cm^{-3}) binding to various surfaces: dependence of bound mass (Γ) per unit area as a function of time (t). +, to GPA to which HSA had been adsorbed; ×, to a bare DMPC-cholesterol membrane; ■, to GPA without HSA; □, to HSA. Only the WGA bound to the GPA-HSA could be removed by GlcNAc; all the WGA could be removed by 56 mM HCl.

Results and discussion

Incorporation of GPA into bilayer lipid membranes

We initially considered preparing DMPC-cholesterol-GPA vesicles as suggested by Ketis *et al.* [35], and using these vesicles to prepare monolayers [43] with which the waveguides could be coated as illustrated in Fig. 1. Since, however, vesicle preparation is a lengthy procedure and there is uncertainty as to the exact concentration of incorporated GPA, we decided to deposit a DMPC-cholesterol bilayer membrane using the Langmuir-Blodgett technique on to the waveguide, and then expose the bilayers to GPA in solution. The following evidence suggests that GPA was correctly inserted into the membrane: (a) only a very small fraction (1–2%) of the GPA could be removed by flushing with pure buffer; (b) the GPA showed specific reactivity towards WGA (see below); (c) GPA could not be removed from the membrane by briefly flushing with 56 mM HCl; (d) when the bilayer membrane was completely removed from the waveguide by slowly (0.27 mm s^{-1}) vertically lowering it into a clean Langmuir trough [44], a residue of protein remained attached to the waveguide surface, implying transmembrane penetration of GPA and attachment of its cytosolic domain to the underlying $Si_{0.55}Ti_{0.45}O_2$ surface. We presume that this attachment neither interferes with oligomerization of GPA nor restricts its orientation within the bilayer, and that the exposed glycosylated terminal domain can adopt a native conformation.

Kinetic analysis of GPA incorporation

The most general formulation of the (irreversible) deposition rate $d\Gamma/dt$ takes the form:

$$d\Gamma/dt = I\,\phi \tag{4}$$

where I is the flux to the empty surface, and ϕ is the 'available area function'. It is not expected that specific binding sites for GPA exist on the DMPC-cholesterol surface, since the lipid head groups are much smaller than the GPA molecules, and the membrane is therefore a quasicontinuum at which the GPA can adsorb. Therefore, in computing ϕ zones excluded from further adsorption by molecules already adsorbed must be taken into account [45]. Calling $\theta = a\Gamma/m$ the fraction of total surface occupied by bound protein, where a and m are respectively the occupied area and mass per molecule, calculation (the random sequential deposition model) gives [45]:

$$\phi = 1 - 4\theta + \frac{6\sqrt{3}}{\pi}\theta^2 + \beta\theta^3, \tag{5}$$

where β = 1.406876. This equation is valid up to $\theta \approx 0.35$. Under our conditions, in which transport of GPA to the DMPC-cholesterol surface is governed by pure diffusion, I is time dependent [46], and expression (4) becomes:

$$d\Gamma / dt^{0.5} = 2g_0(D_g/\pi)^{0.5}\phi, \tag{6}$$

where g_0 is the bulk solution protein concentration and D_g the diffusion coefficient of GPA. Figure 5 shows the result of the fit of equation (6) to the experimental Γ_{GPA} versus t data, plotted as $d\Gamma_{GPA}/dt$ versus Γ_{GPA}, with best parameters m/a = 0.35 μg cm^{-2} and $D_g = 1.5 \times 10^{-8}$ cm^2 s^{-1}.

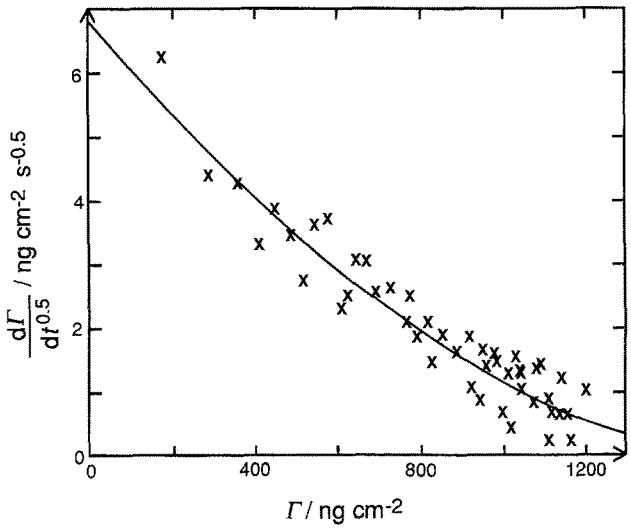

Figure 5. Analysis of the GPA-membrane interaction. The data from Fig. 3 has been used to determine Γ_{GPA} which is plotted according to equations (6), (5) and (4) (crosses). Full line: equation (6) with c_b = 50 μg cm^{-3}, a/m = 2.8 cm^2 μg^{-1} and $D_g = 1.5 \times 10^{-8}$ cm^2 s^{-1}.

In an unstirred, diffusion-controlled system the flux of molecules to the surface becomes very slow as time passes [46], and it is difficult to assess whether an apparent adsorption plateau is reached due to the deceleration of the flux or to the saturation of the surface available for adsorption. Hence, we repeatedly renewed the solution in the cuvette with fresh aliquots of GPA, until no further change in the adsorbed mass was apparent. In this way we could adsorb 148 ng cm^{-2}, of which less than 2% was removed by flushing with pure buffer. Complete monolayer coverage would equal m/a, i.e. 0.35 μg cm^{-2} (see above); hence we could adsorb 42% of a complete monolayer. Maximum possible adsorption is about 55% [47] of complete monolayer coverage, i.e. 0.196 μg cm^{-2}. It is not too surprising that we failed to reach the theoretical limit, since filling of the surface becomes asymptotically slow for $\theta > 0.4$ [48], the reason being that very few gaps large enough to accept another molecule remain. This feature of random sequential deposition ensures that the DMPC-cholesterol surface (for which WGA has some affinity) is effectively inaccessible to WGA in solution once the GPA has been adsorbed.

A major point of current uncertainty concerns the state of oligomerization of GPA in the membrane. If GPA is a dimer, it has an approximate molecular weight of 76 kDa. Taking the

partial specific volume to be 0.74 $cm^3\ g^{-1}$, the same as for bovine serum albumin [49], and assuming the molecule to be roughly spherical, we obtain a radius of 28 Å, an *m/a* ratio of 0.5 $\mu g\ cm^{-1}$, and, using the Stokes-Einstein equation, $D_g = 8.7 \times 10^{-7}\ cm^2\ s^{-1}$. These values appear to be incompatible with our data, however – they result in a curve somewhat off the upper right-hand corner of Fig. 5. We should point out that the diffusion coefficient determined from our experimental data carries the assumption that every GPA molecule arriving at the bilayer is successfully incorporated. Since a particular part of the molecule has to insert itself into the bilayer, this is highly improbable. Presumably only molecules of a certain orientation with respect to the bilayer are able to insert successfully, in which case the overall rate of insertion will be substantially less than the diffusion-limited rate, assuming that the molecules approach the membrane oriented at random [50]. This effect results in an apparent diffusion coefficient less than for self-diffusion in dilute solution. Furthermore, we have neglected electrostatic effects: the DMPC-cholesterol membrane is initially electrically neutral but GPA is expected to be highly negative due to the sialic acid in the extensively glycosylated extracellular domain. Therefore, as GPA becomes incorporated into the membrane, it will increasingly repel fresh GPA molecules arriving from the solution. This repulsion will also diminish the apparent diffusion coefficient. Without analysing these factors in more detail, it is premature to draw conclusions about the shape or size of the GPA molecule from the experimentally determined apparent diffusion coefficient. Regarding the other parameter, *m/a*, we note that a two-dimensional monomer cluster of any size would have $m/a = 0.4\ \mu g\ cm^{-2}$, to which our experimentally determined value is fairly close.

Binding of WGA to GPA

A fixed number of GPA binding sites, S, per unit area are available at this stage, and

$$S = \Gamma_{GPA}/m \tag{7}$$

The Langmuir formalism is basically applicable, but must be modified to take account of the following observed features; (i) the adsorption is not completely reversible – after flushing with pure buffer an irreversibly bound residue remains (see Figs 3 and 5); and (ii) the irreversibly bound residue could almost completely be removed by briefly flushing with 0.1 M GlcNAc (Fig. 5).

The binding between oligomeric WGA and possibly oligomeric GPA receptors is potentially highly complex. The starting point of our analysis is to examine some of the kinetic consequences of a simple model suggested by extant literature data. Initially let there be two sites present on the GPA receptor (which may be composed of two or more monomers) with equivalent inherent affinities for WGA. These two target sites are not independent, but show positive cooperativity, that is, that the affinity of the second site increases after the first one has been filled. As mentioned in the Introduction, there is good crystallographic evidence for inter-molecular structure which could be responsible for cooperative linkages. The corresponding reaction scheme is (denoting GPA as G and WGA as W):

$$G + W \underset{k_{-1}}{\overset{k_1}{\rightleftharpoons}} B_1 \tag{8a}$$

$$B_1 + W \underset{k_{-2}}{\overset{k_2}{\rightleftharpoons}} B_2 \tag{8b}$$

where B_1 and B_2 denote respectively complexes in which either or both GPA receptor sites are occupied by WGA. Positive cooperativity implies that

$$K_{a,1} = \frac{k_1}{k_{-1}} < K_{a,2} = \frac{k_2}{k_{-2}}. \tag{9}$$

Determination of the off rates (Fig. 6) If $k_{-2} \ll k_{-1}$, then the plateau observed after washing with pure buffer corresponds to the residual population of B_2. Since we never observed further removal of protein despite moderately prolonged washing, we can put an upper limit on k_{-2}, i.e. $k_{-2} < k_{-1}/100$. Hence during washing for relatively short periods, we have

$$dw_g/dt = db_1/dt = -k_{-1}b_1 \tag{10}$$

where w_g is the total concentration of WGA bound to GPA, i.e.

$$w_g = b_1 + 2b_2, \tag{11}$$

and b_1 and b_2 the concentrations of B_1 and B_2. We cannot directly distinguish between lectins bound to B_1 and B_2: we measure w_g. The solution of equation (10) is:

$$w_g = w_g^* \exp(-k_{-1}t) + 2b_2, \tag{12}$$

where w_g^* denotes the value of w_g just before the start of washing, i.e. the washing curve should be a pure exponential with time constant k_{-1}. The upper decay shown in Fig. 6 is indeed a pure exponential, not to zero bound mass, but to an intermediate value equal to $2b_2$. In the case of WGA bound to GPA-HSA, this behaviour reflects the existence of two distinct binding sites. The mean value of the rate constant k_{-1} fitted to the dissociation curves is $2.7 \pm 0.2 \times 10^{-3}\ s^{-1}$.

Determination of the on rates During protein binding the transport is purely diffusion controlled, and the flux I towards the surface is given by:

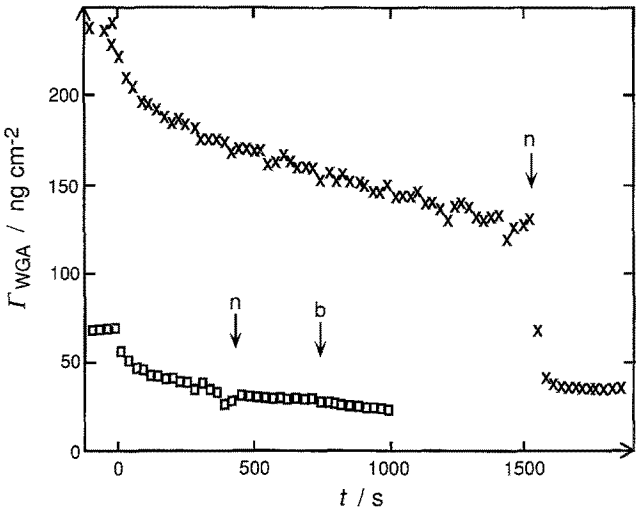

Figure 6. Removal of WGA from membrane-bound GPA by flushing with pure buffer (flushing began at $t = 0$, and at the point marked with arrow b) and with GlcNAc (marked with arrows n). ×, WGA bound to GPA-HSA; □, WGA bound to GPA alone.

$$I = (w_0 - w_s)\sqrt{\frac{D_w}{\pi t}} \tag{13}$$

where w is the concentration of WGA, subscripts 0 and s denoting the bulk and near surface concentrations, and D_w the diffusion constant of WGA. The near-surface concentration term arises because the surface carrying GPA is not a perfect sink for WGA. The net rate of binding is then given by the sum of:

$$db_1/dt = k_1 w_s \theta_0 - k_{-1} b_1 - k_2 w_s \theta_1 + k_{-2} b_2 \tag{14}$$

and

$$db_2/dt = k_2 w_s \theta_1 - k_{-2} b_2 \tag{15}$$

θ_0, θ_1, and θ_2 denote the fractions of the total number of sites S occupied by 0, 1 and 2 WGA molecules, i.e.

$$\begin{aligned} \theta_0 &= 1 - \frac{b_1}{m_w S} - \frac{b_2}{m_w S} \\ \theta_1 &= \frac{b_1}{m_w S} \\ \theta_2 &= \frac{b_2}{m_w S} \end{aligned} \tag{16}$$

where m_w is the mass of one molecule of WGA. To find w_s, we apply the steady state condition, $dw_s/dt \approx 0$, and hence $I = dw_g/dt$. By differentiating equation (11) and substituting in equations (13–15), we obtain, after rearrangement,

$$w_s = \frac{w_0 (D/\pi t)^{0.5} + k_{-1} b_1}{(D/\pi t)^{0.5} + k_1 \theta_0 + k_2 \theta_1}, \tag{17}$$

where we have dropped the term $k_{-2}b_2$, since $k_{-2} \ll k_{-1}$ while b_1 and b_2 are comparable. Equations (16) and (17) allow (14) and (15) to be expressed as two simultaneous differential equations in the two unknowns b_1 and b_2. A numerical solution fitted to our experimental data yielded values of 5.4×10^{-5} and 9.6×10^{-7} cm s^{-1} for k_1 and k_2 respectively. To convert this quantity expressed in heterogeneous units to the more familiar homogeneous ones ($M^{-1}s^{-1}$) we have to multiply by $4\pi N_A r^2/1000$ [51], where N_A is Avogadro's number and r the radius of the WGA molecule, which we take to be 2.2 nm for the dimer, obtaining $k_1 = 2.0 \times 10^4$ M^{-1} s^{-1} and $k_2 = 3.5 \times 10^2$ M^{-1} s^{-1}. From this and the values we determined and estimated for the off rates (respectively $k_{-1} = 2.7 \times 10^{-3}$ s^{-1} and $k_{-2} < 10^{-5}$ s^{-1}) we calculate $K_{a,1}$ (low-affinity site) = 7.4×10^6 M^{-1} and $K_{a,2}$ (high-affinity site) $\geqslant 4 \times 10^7$ M^{-1}. These values are in good agreement with those determined previously from binding isotherms [7, 15]. Note that the 'low-affinity' site actually has a smaller on rate than the high affinity site; the positive cooperativity arises from a large difference in the off rates.

Stoichiometry of GPA-WGA association The stoichiometry S was determined according to

$$S = \frac{\Gamma_{WGA}}{\Gamma_{GPA}} \cdot \frac{M_{GPA}}{M_{WGA}} \tag{18}$$

where M refers to molecular weights. As noted above, by repeated addition of GPA solution we could load the membrane with 148 ng cm^{-2} of GPA. Following saturation with HSA, by repeated addition of WGA we could bind 271 ng cm^{-2} of WGA to the GPA. According to equation (18), using *monomer* molecular weights of 38 and 17.5 kDa for GPA and WGA respectively, we obtain a stoichiometry of 4.0 (± 0.2) WGA monomers per GPA monomer. This value represents merely an average, as it is not presently known what type of GPA aggregates are present in the bilayer. Thus, whether two WGA dimers bind to the same bivalent oligosaccharide in a cross-linking mode, or whether each WGA dimer binds to distinct oligosaccharides on a given GPA monomer is indeterminate. However, it is noteworthy that this stoichiometry is in good agreement with that found by Lovrien and Anderson, who carried out their binding studies with intact cells. These authors concluded that interlinkage of WGA dimers by GPA receptors was the most likely interpretation of their data [15].

Effect of adding GlcNAc During washing we observed that the population of WGA molecules bound to the higher affinity site is kinetically stable. Nevertheless, the addition of excess GlcNAc causes nearly all this bound WGA to be released very rapidly (see Fig. 6). This result is suggestive of an allosteric effect, because competitive replacement of GPA by GlcNAc would otherwise be limited by the off rate k_{-2}, which we have found to be smaller than 10^{-5} s^{-1}. Since it is evident from the binding stoichiometry that not all 8 potential binding sites of a given WGA dimer are involved in the binding to GPA,

GlcNAc may bind to some of the unoccupied WGA sites, at least initially, thereby triggering dissociation by a mechanism other than competitive binding to the same high affinity sites utilized in the WGA-GPA complex.

Possible binding interactions in terms of the molecular structure of WGA It is well established that sialic acid, which resides at the non-reducing termini of all oligosaccharide moieties on GPA, mediates the binding interactions with WGA. This is substantiated by the fact that enzymatic removal of sialic acid from red cell membranes dramatically reduces the apparent association constants for the two classes of binding sites [7] that were predicted, and abolishes the profound controlling effect WGA exerts on the interconversion of discrete erythrocyte morphologies [15].

Three independent binding sites have been characterized in the crystal structure of WGA complexed with the tryptic GPA sialoglycoöctapeptide T5, bearing a branched bivalent O-linked tetrasaccharide. The three sites differ in their chemical environments and thus possess different affinities towards NeuNAc. One site showed only weak binding, but NeuNAc bound at this site was found to be involved in a crucial lattice contact. The other two sites were highly occupied and utilized in an ordered crosslinked lattice network. In this binding mode the non-reducing NeuNAc residues at opposite ends of the extended tetrasaccharide interlink WGA dimers [18]. Each NeuNAc binds to a distinct site on a different monomer in each of the interlinked dimers which approach to within 15Å. Both these sites are presumed to be the high affinity sites of WGA, even though they have different aromatic residues. It is important to note that in each crosslinked dimer the domain-B site is occupied only in monomer 1 and the domain-C site only in monomer 2; the domain-B site in monomer 2 and the domain-C site in monomer 1 remain vacant and are involved in lattice contacts. Considering the binding stoichiometries observed by Lovrien and Anderson [15] and in our binding studies, such a model may thus have physiological relevance. A binding mode in which GPA molecules are interlinked by WGA is unlikely, as GPA receptors in the erythrocyte membrane are separated by 220Å [15], a distance much too large for a single WGA molecule of about 50Å diameter to bridge.

The observation that only three of the six possible binding sites for NeuNAc are utilized on the WGA dimer in this crosslinked complex has raised the interesting possibility that multivalent lectins may use only some of their binding sites in binding to complex cell surface receptors [18]. It is well documented that lectin binding sites involved in inter-molecular lattice contacts are inaccessible to saccharide. However, as shown by soaking experiments of WGA-T5 crystals [19], some of these sites may be accessible to externally added monosaccharide. For example, NeuNAc binds to only one of the vacant sites, the high affinity domain-B site, and does not destabilize the crystal lattice. In contrast, GlcNAc slowly breaks up the crystal lattice. It presumably binds to sites which are involved in lattice contacts (domain-D site). Thus, based on this structural evidence for a possible mode of WGA-receptor interaction, we suggest that the rapid lectin-receptor dissociation resulting from exposure to monosaccharide may occur by an allosteric mechanism. That is, GlcNAc is unlikely to compete with the high affinity receptor sites, but rather binds to vacant high or low affinity sites, which may be loosely involved in lectin self-interactions that stabilize ordered aggregates. This would have the effect of destabilizing the GPA-WGA complex and result in its dissociation.

Concluding remarks

The results reported here on the specific interaction of WGA with its membrane receptor GPA are consistent with earlier reported data and structural evidence based on a WGA-sialoglycopeptide crystal structure. Our data clearly show: (i) that two types of binding sites are involved when WGA binds to GPA incorporated into a lipid bilayer, confirming previous results, and (ii) that the high affinity site actually has a somewhat smaller on rate than the low affinity site, and a much smaller off rate. WGA bound to the high affinity site can be rapidly released by the addition of GlcNAc, however, suggesting an allosteric mechanism with sugar binding at another site.

The binding stoichiometry of 4:1 (WGA:GPA) supports the earlier conclusion of Lovrien and Anderson that WGA molecules are cross-linked by GPA receptors. However, we cannot yet provide information on the oligomeric state of GPA or on the degree of homogeneity of the intermolecular interactions that stabilize the WGA-GPA complex.

A supported planar phospholipid bilayer is a well-characterized model membrane system for the study of receptor-membrane and ligand-receptor interactions, free from the complexities which render the interpretation of data for binding to the cell surface problematical. Here we have developed a framework based on interpreting kinetic binding data. Given the lengthy times for equilibration in this system, and the novel possibilities of obtaining very accurate kinetic data using the integrated optical technique, the kinetic approach is capable of yielding new insights into lectin-receptor interaction mechanisms. Compared with the evaluation of equilibrium binding isotherms by Scatchard analysis, we are now in a much stronger position to analyse subtle aspects of complex interactions that formerly could not have been dealt with.

Acknowledgements

It is a pleasure to thank Mr Leo Faletti for his skilful construction of the Langmuir trough, Dr Gernot Hänisch and Mr Franz Biry for the design and construction of the accompanying electronic control equipment, and the Human Frontier Science Program Organization for financial support.

References

1. Nicolson GL (1974) *Int Rec Cyt* **39**:89–190
2. Lis H, Sharon N (1981) In *The Biochemistry of Plants: A Comprehensive Treatise, Proteins and Nucleic Acids.* (Marcus A, ed.) **Vol. 6**: pp. 371–447. New York: Academic Press.
3. Goldstein IJ, Poretz RD (1986) In *The Lectins: Properties, Function, and Application in Biology and Medicine* (Liener IE, Sharon N, Goldstein IJ, eds) pp. 43–247. Orlando, FL: Academic Press.
4. Sharon N, Lis H (1975) *Methods Membr Biol* **3**:147–200.
5. Lis H, Sharon N (1977) *The Antigens* **4**:464–529.
6. Scatchard G (1949) *Ann N Y Acad Sci* **51**:660–72.
7. Adair WL, Kornfeld S (1974) *J Biol Chem* **249**:4696–704.
8. Obrenovitch A, Sene C, Roche AC, Monsigny M, Visher P, Hughes RC (1981) *Biochimie* **C3**:169–75.
9. Cuatrecasas P (1973) *Biochemistry* **12**:1312–23.
10. Bornens M, Karsenti E, Acrameas S (1976) *Eur J Biochem* **65**:61–69.
11. Reisner Y, Lis H, Sharon N (1976) *Exp Cell Res* **97**:445–48.
12. Stanley P, Carver JP (1977) *Proc Natl Acad Sci USA* **74**:5056–59.
13. Purjanski A, Ravid A, Sharon N (1978) *Biochim Biophys Acta* **508**:137–46.
14. Gordon JA, Young RK (1979) *J Biol Chem* **254**:1932–37.
15. Lovrien RE, Anderson RA (1980) *J Cell Biol* **85**:534–48.
16. Bhattacharyya L, Fant J, Lonn H, Brewer CF (1990) *Biochemistry* **29**:7523–30.
17. Bhattacharyya L, Brewer CF (1992) *Eur J Biochem* **208**: 179–85.
18. Wright CS (1992) *J Biol Chem* **267**:14345–52.
19. Wright CS, Jaeger J (1993) *J Mol Biol* **232**:620–38.
20. Weis WI, Drickamer K, Hendricksen WA (1992) *Nature* **360**:127–34.
21. Bhavanandan VP, Katlic AW (1979) *J Biol Chem* **254**:4000–8.
22. Peters BP, Ebisu S, Goldstein IJ, Flashner M (1979) *Biochemistry* **18**:5505–11.
23. Monsigny M, Roche A-C, Sene C, Maget-Dana R, Delmotte F (1980) *Eur J Biochem* **104**:147–53.
24. Ganguly P, Fosett NG (1981) *Blood* **57**:343–52.
25. Johnson RJ, Simpson S, Van Epps DE, Chenoweth DE (1992) *J Leukocyte Biol* **52**:3–10.
26. Tomita M, Marchesi VT (1975) *Proc Natl Acad Sci USA* **72**:2964-68.
27. Thomas DB, Winzler RJ (1969) *J Biol Chem* **244**:5943–46.
28. Irimura T, Tsugi T, Tagami S, Yamamoto K, Osawa E (1981) *Biochemistry* **20**:560–66.
29. Yoshima H, Furthmayr H, Kobata A (1980) *J Biol Chem* **255**:9713–18.
30. Springer GF, Nagai Y, Tegtmeyer H (1966) *Biochemistry* **5**:3254–72.
31. Enegren BJ, Burness ATH (1977) *Nature* **268**:536–37.
32. Wright CS (1987) *J Mol Biol* **194**:501–29.
33. Grant CWM, McConnell HM (1974) *Proc Natl Acad Sci USA* **71**:4653–57.
34. Sharom FJ, Barrat DG, Grant CWM (1977) *Proc Natl Acad Sci USA* **74**:2751–55.
35. Ketis NV, Girdlestone J, Grant CWM (1980) *Proc Natl Acad Sci USA* **77**:3788–90.
36. Ramsden JJ (1993) *J Statist Phys* **73**:853–77.
37. Roberts GG (1990) *Langmuir-Blodgett Films.* New York: Plenum.
38. Poste G, Moss C (1972) *Prog Surf Sci* **2**:139–232.
39. Schaaf P, Dejardin PH, Schmitt A (1985) *Rev Phys Appl* **20**:631–40.
40. Wright CS (1981) *J Mol Biol* **145**:453–61.
41. Tiefenthaler K, Lukosz W (1989) *J Opt Soc Am B* **6**:209–20.
42. de Feijter JA, Benjamins J, Veer FA (1978) *Biopolymers* **17**:1759–72.
43. Schindler H (1980) *FEBS Lett* **122**:77–79.
44. Langmuir I (1919) *Trans Faraday Soc* **15**:62–74.
45. Schaaf P, Talbot J (1989) *J Chem Phys* **91**:4401–9.
46. von Smoluchowski M (1916) *Phys Z* **17**:557–99.
47. Hinrichsen EL, Feder J, Jøssang T (1986) *J. Statist Phys* **44**:793–827.
48. Swendsen R (1981) *Phys Rev A* **24**:504–8.
49. Charlwood PA (1957) *J Am Chem Soc* **79**:776–81.
50. Schurr JM, Schmitz KS (1976) *J Phys Chem* **80**:1934–36.
51. Armstrong FA, Hill HAO, Walton NJ (1986) *Q Rev Biophys* **18**:261–322.